

The Umov effect applied to single particles

E. Zubko^{*,1,2}, G. Videen³, Yu. Shkuratov², K. Muinonen^{1,4}, and T. Yamamoto⁵

¹*Department of Physics, P.O. box 64, FI-00014 University of Helsinki, Finland.*

²*Institute of Astronomy, Kharkov National University, 35 Sumskaya St., Kharkov, 61022, Ukraine.*

³*Space Science Institute, 4750 Walnut Street, Suite 205, Boulder, CO 80301 USA.*

⁴*Finnish Geodetic Institute, P.O. box 15, FI-02431 Masala, Finland.*

⁵*Institute of Low Temperature Science, Hokkaido University, Kita-ku North 19 West 8, Sapporo 060-0819, Japan.*

We study the Umov effect as applied to single irregularly shaped particles comparable with wavelength. For these particles an inverse correlation between geometric albedo and maximum of positive polarization at large phase angles does exist; however, it takes a form different from what was found for planetary regoliths. The difference is substantially caused by contribution of relatively small particles with $x < 14$.

INTRODUCTION

The Umov effect refers to the inverse correlation between geometric albedo (albedo_G) and the amplitude of the maximum of linear polarization (P_{\max}) of sunlight scattered from rough surfaces. It is being exploited in astronomical studies of the Solar system objects, such as asteroids, atmosphereless planets, and moons. This correlation is valid over a wide range of albedo (e.g., [1]), including relatively dark objects, like the Moon, whose average albedo is about 12%. For such dark surfaces, one expects a relatively small contribution of multiple scattering between constituent particles and a greater role of the first scattering order than for brighter objects. Therefore, one can extrapolate that if a dark regolith shows the Umov effect, then single constituent particles forming that regolith should show the effect, too.

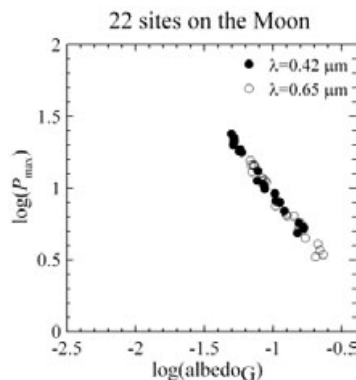


Figure 1. Diagram $\log(P_{\max})$ vs. $\log(\text{albedo}_G)$ for 22 sites on the Moon [1].

* Corresponding author: Evgenij Zubko (ezubko@rambler.ru)

One unknown is the mathematical relationship the Umov effect takes in the case of single dust particles comparable with the wavelength. In the case of a regolith, a linear relation exists between $\log(P_{\max})$ and $\log(\text{albedo}_G)$. Figure 1 shows such a diagram for 22 various sites of the Moon (data adopted from [1]).

TECHNIQUE AND DETAILS OF CALCULATION

We compute light-scattering properties of irregularly shaped particles using the discrete dipole approximation (DDA) (e.g. [2]), and we use the algorithm developed by Zubko et al. [3]. We consider agglomerated debris particles, whose generation is described in [3]. These irregular particles are fluffy in nature, having a material density of approximately 25 % of the volume of a circumscribing sphere. Note that such features are thought to be quite relevant for a model of cosmic dust and regolith particles. We consider light-scattering properties that are well averaged over sample shapes; in each case, at least 500 shapes have been considered. In many cases this number is significantly larger to make the results statistically reliable. Detail on averaging can be found in [3]. We consider homogeneous materials having one of 15 different refractive indices m , representative of materials in cometary dust and regoliths of atmosphereless celestial bodies: $m = 1.2 + 0i$, $1.313 + 0i$, $1.313 + 0.1i$, $1.4 + 0i$, $1.5 + 0i$, $1.5 + 0.02i$, $1.5 + 0.1i$, $1.6 + 0.0005i$, $1.6 + 0.01i$, $1.6 + 0.02i$, $1.6 + 0.05i$, $1.6 + 0.1i$, $1.7 + 0i$, $1.7 + 0.1i$, and $1.758 + 0.0844i$. We classify all these materials into two groups for convenience: highly absorbing ($\text{Im}(m) > 0.02$) and weakly absorbing ($\text{Im}(m) \leq 0.02$) materials. Another parameter important for light scattering is the size parameter $x = 2\pi r/\lambda$, where r is the radius of the circumscribing sphere and λ is the wavelength of the incident radiation. Through this study, the size parameter x has been varied from 2 to 40.

RESULTS AND DISCUSSION

The definition of albedo for single particles is different from that of regoliths. Indeed, the geometric albedo does not specify absorption or scattering efficiency: $\text{albedo}_G = (S_{11} \pi) / (k^2 G)$, where S_{11} is the total intensity Mueller matrix element at backscattering, k is the wavenumber, and G is the geometric cross-section of the particle. Instead, it describes only the efficiency of backscattering. The use of single-scattering albedo seems a more reasonable choice for analysis, since it includes the total scattering and not that at an arbitrary angle. In [3] it was shown that the amplitude of positive polarization was inversely correlated with single-scattering albedo over a wider range of $\text{Im}(m)$ than the geometric albedo. However, the use of the single-scattering albedo meets an obvious difficulty when non- or weakly absorbing particles are considered. Indeed, for $\text{Im}(m) = 0$, the single-scattering albedo equals to unity throughout the entire range of size parameter x ; whereas, the amplitude of positive polarization dramatically varies over x .

In the upper row of Fig. 2, the diagrams of P_{\max} versus the single-scattering albedo are shown; whereas, the bottom row displays similar diagrams for the case of the geometric al-

bedo. The subscripts “S” and “G” designate single-scattering and geometric albedos, respectively. In both cases, the left panel corresponds to highly absorbing materials; whereas, the right panel corresponds to weakly absorbing materials. Arrowed lines show the dependence on the size parameter x . As one can see from Fig. 2, there exists a much stronger inverse correlation of P_{\max} with the geometric than the single-scattering albedo, especially for weakly absorbing particles (right bottom panel). In all cases, the relationship depends on the particle size, and only for weakly absorbing particles does there appear to be a functional dependence on P_{\max} with albedo_G . No functional dependence appears between P_{\max} with albedo_S ; thus, we consider and discuss only the inverse correlation of P_{\max} with albedo_G .

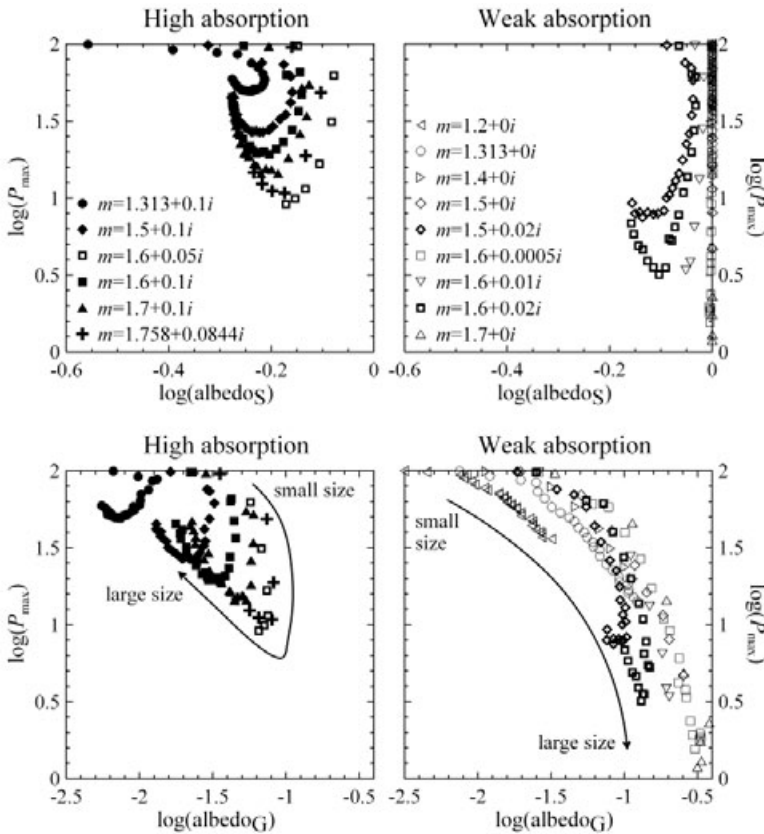


Figure 2. Diagrams $\log(P_{\max})$ vs. $\log(\text{albedo}_S)$ (upper row) and $\log(P_{\max})$ vs. $\log(\text{albedo}_G)$ (bottom row) for agglomerated debris particles.

When we consider highly absorbing particles, an inflection is clearly seen in the bottom left panel in Fig. 2. One also can be found in the bottom right panel for the cases of $m = 1.5 + 0.02i$ and $m = 1.6 + 0.02i$. These inflection points depend on the real part of refractive index $\text{Re}(m)$; for instance, at $\text{Im}(m) = 0.1$, when varying $\text{Re}(m)$ from 1.313 to 1.7, the size parameter of the inflection decreases from about $x = 18$ to 10. The inflection strongly depends also on $\text{Im}(m)$. For example, at $\text{Re}(m) = 1.6$, when varying $\text{Im}(m)$ from 0.02 to 0.1 only, its size parameter is decreased from $x = 16$ to 10. A detection of this inflection point on the $P_{\max} - \text{albedo}_G$ diagram could be used to retrieve properties of target particles. Such a possi-

bility is especially intriguing for cometary dust particles that are thought to be highly absorbing.

The inverse correlation between $\log(P_{\max})$ and $\log(\text{albedo}_G)$ in Fig. 2 is obviously non-linear. For highly absorbing particles, a minimum appears when the particles are approximately $x = 14$. For larger particles, the relationship is nearly linear. In Fig. 3 we show the combined results of highly and weakly absorbing particles $x > 14$ in the left panel. In the right panel we show just the particles having $x = 14$. In this case, the trend for highly absorbing particles can be distinguished from that for weakly absorbing particles.

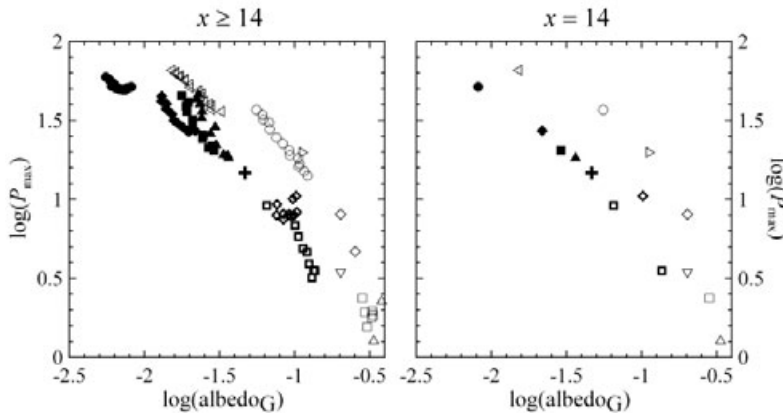


Figure 3. Diagrams $\log(P_{\max})$ vs. $\log(\text{albedo}_G)$ for agglomerated debris particles.

Finally, we note that variations of the refractive index m cause the trend line to move on the $\log(P_{\max}) - \log(\text{albedo}_G)$ diagrams; whereas, the scatter from this trend line due to variations of the size parameter x are relatively small (compare left and right panels in Fig. 3). This result can potentially assist in characterizing particle composition.

REFERENCES

- [1] Yu.G. Shkuratov and N.V. Opanasenko. Polarimetric and photometric properties of the Moon: Telescopic observations and laboratory simulations: 2. The positive polarization. *Icarus* **99** (1992).
- [2] B.T. Draine and P.J. Flatau. Discrete-dipole approximation for scattering calculations. *JOSA A* **11** (1994).
- [3] E. Zubko, H. Kimura, Yu.G. Shkuratov, K. Muinonen, T. Yamamoto, H. Okamoto, and G. Videen. Effect of absorption on light scattering by agglomerated debris particles. *JQSRT* **110** (2009).